ANALYSIS OF NONLINEAR CELLULAR DYNAMICS IN THE COCHLEA USING THE CONTINUOUS WAVELET TRANSFORM AND THE SHORT-TIME FOURIER TRANSFORM

Conor Heneghan [1] *Malvin C. Teich* [1] *Shyam M. Khanna* [2] *Mats Ulfendahl* [3]

[1] Department of Electrical Engineering, Columbia University, New York, NY 10027
[2] Department of Otolaryngology, Columbia College of Physicians & Surgeons, New York, NY 10032
[3] Department of Physiology and Pharmacology, Karolinska Institutet, S17177 Stockholm, Sweden

ABSTRACT

The Continuous Wavelet Transform (*CWT*) and the Short-Time Fourier Transform (*STFT*) are used to analyze the time course of cellular motion in the guinea-pig inner ear. The velocity responses of individual auditory cells (outer hair cells and Hensen's cells) to amplitude-modulated (*AM*) acoustical signals display characteristics typical of nonlinear systems, such as harmonic generation. Nonlinear effects are particularly pronounced at the highest stimulus levels, where half-harmonic, and sometimes quarter-harmonic, components are also seen. Both the *CWT* and the *STFT* are found to be useful in analyzing these velocity responses. We carry out *CWT* analyses using a Morlet wavelet and an *AM* wavelet, and find the results are quite similar.

1. INTRODUCTION

The velocity of vibration of cellular structures in the guinea-pig cochlea has been measured by using laser-heterodyne interferometry [1]. The Short-Time Fourier Transform (*STFT*) is a useful tool for following the time course of the frequency components generated in response to an amplitude-modulated (*AM*) stimulus. *STFT* analysis has revealed that the cellular vibrations are strongly nonlinear: they exhibit spectral components not only at the carrier frequency of the *AM* stimulus f_c, but at its harmonics, half-harmonics, and even quarter-harmonics [2]-[5]. In this paper, we show that the Continuous Wavelet Transform (*CWT*) [6] is similarly useful, and both the *CWT* and the *STFT* are used to demonstrate the presence of components at quarter-harmonic frequencies. The presence of quarter-harmonic as well as half-harmonic and harmonic spectral components indicate that the system may undergo a period-doubling route to chaos [5].

2. METHODS

The *CWT* and *STFT* of the measured velocity response were calculated. The *CWT* of a signal $x(t)$ is defined as

$$CWT_x^h(r,\tau) = \frac{1}{\sqrt{|r|}} \int_{-\infty}^{+\infty} x(t) h^* \left(\frac{t-\tau}{r}\right) dt, \qquad (1)$$

with r as a scale variable, τ as a time variable, $x(t)$ as the velocity signal to be analyzed, $h(t)$ as the prototype wavelet basis function, and * denoting complex conjugation. This can also be written as an integral in the frequency domain, *viz.* [5]

$$CWT_x^h(r,\tau) = \sqrt{|r|} \int_{-\infty}^{\infty} X(u) H^*(ur) \exp(j2\pi u\tau) du, \quad (2)$$

where u is a dummy frequency variable, and $X(u)$ and $H(u)$ represent the Fourier transforms of $x(t)$ and $h(t)$, respectively.

The fast-*CWT* algorithm of Jones and Baraniuk [7] was used to calculate a discrete approximation of (1). For comparison, we calculated the *CWT* based on two different analysis wavelets; a Morlet wavelet [8] and an *AM* wavelet. The discrete-time prototype Morlet wavelet was obtained by sampling the continuous Morlet wavelet $h_M(t) = \exp(jct)\exp(-\alpha t^2/2)$ (with $c = 4750$ and $\alpha = 12207$) at 5000 Hz, the sampling rate of the original data set. The discrete-time prototype *AM* wavelet was obtained by sampling the continuous wavelet $h_{AM}(t) = R_{1/2f_m}(t)\exp(j2\pi f_c t)[1+\cos(2\pi f_m t)]/2$, where $R_T(t)$ denotes the indicator function on the interval $[-T,T]$, and with $f_c = 756$ and $f_m = 21.0$.

These wavelets were chosen inasmuch as their relative bandwidths (BW_{rel}) are readily controlled. Relative bandwidth is defined as the full-width (Δf) at $1/e$ maximum of the bandpass region surrounding the center frequency of the wavelet's Fourier transform, divided by the center frequency itself (*i.e.*, $BW_{rel} = \Delta f/f$). Since the frequency resolution of the *CWT* at scale r is usefully defined as the frequency width of $H(ur)$, controlling the relative bandwidth is equivalent to controlling the desired frequency resolution at a given analysis frequency f. In our case, the relative bandwidths of the Morlet wavelet and the *AM* wavelet are $2\sqrt{2\alpha}/c$ and $2.36 f_m/f_c$, respectively. Our choice of parameters for the Morlet and *AM*-based wavelets is such that they have the same relative bandwidths.

The *CWT* is strictly defined as a time–scale representation; however it often proves easier to interpret *CWT*s in terms of time and frequency rather than time and scale. A short-lived function (r small) inherently contains high frequencies, so that r is inversely related to frequency. For a given wavelet transform, the mapping $f = K/r$ can be used, allowing the *CWT* of a signal to be interpreted in terms of frequency rather than scale. We have chosen $K = 756$. We readily note from (2) that, unlike the *STFT*, the *CWT* does

0-7803-2127-8/94 $4.00 ©1994 IEEE

not map equal-amplitude sinusoidal components into equal-magnitude CWTs because of the premultiplication factor of $\sqrt{|r|}$ in the definition. To facilitate comparison between the $STFT$ and the CWT, we therefore plot $|r|^{-1/2}CWT$, which we refer to as the "modified CWT".

The $STFT$ of a signal $x(t)$ is defined as

$$STFT_x^g(f,\tau) = \int_{-\infty}^{\infty} x(t)g^*(t-\tau)\exp(-j2\pi ft)\ dt, \quad (3)$$

with f as a frequency variable, τ as a time variable, and $g(t)$ as a window function in time. This can also be written as an integral in the frequency domain, *viz.* [5]

$$STFT_x^g(f,\tau) = \quad (4)$$
$$\exp(-j2\pi f\tau)\int_{-\infty}^{\infty} X(u)G^*(u-f)\exp(j2\pi u\tau)\ du,$$

where $X(u)$ and $G(u)$ represent the Fourier transforms of $x(t)$ and $g(t)$, respectively, and u is a dummy frequency variable. The Gaussian window $g(t) = \exp(-\beta t^2/2)$ (with $\beta = 12207$) was chosen. A discrete approximation of the $STFT$ was calculated by taking the Fast Fourier Transforms of windowed sections of the sampled velocity waveform [2]-[5]. The discrete-time window was obtained by sampling the Gaussian window at 5000 Hz.

3. RESULTS

Figure 1(a) shows the velocity waveform of a third-turn outer hair cell in response to an AM pulse (modulation index = 100%; modulation frequency = 2.44 Hz) with a carrier frequency f_c = 756 Hz. This frequency lies at the characteristic frequency (CF) of the cell, *i.e.*, at the acoustic frequency to which the cell responds maximally. The peak sound intensity of the stimulus at the tympanic membrane was 134 dB:re .0002 dynes/cm^2 (uncorrected). The velocity waveform is seen to be highly irregular. The modified CWT magnitude (calculated using the Morlet wavelet) of this waveform is shown in 3D format in Fig. 1(b) and in 2D contour format in Fig. 1(c). The frequency resolution of this CWT is 49.7 Hz at an analysis frequency of 756 Hz. The CWT comprises components at harmonic (f_c, $2f_c$, and $3f_c$), half-harmonic ($f_c/2$, $3f_c/2$, and $5f_c/2$), and quarter-harmonic ($3f_c/4$, $5f_c/4$, $7f_c/4$, and $9f_c/4$) frequencies. The widths of the spectral components increase as we go to higher analysis frequencies, since the CWT's frequency resolution becomes increasingly worse at those frequencies. In passing, we note that the Morlet wavelet is not strictly admissible [6, 8] since $H_M(0) \neq 0$, where H_M denotes the Fourier transform of $h_M(t)$.

The modified CWT magnitude calculated using the AM wavelet, for the same waveform, is shown in 3D format in Fig. 1(d) and in 2D contour format in Fig. 1(e). These are difficult to distinguish from the Morlet results shown in Figs. 1(b) and 1(c), respectively. This is not surprising inasmuch as the AM-wavelet-based and the Morlet-wavelet-based analyses were chosen to have the same frequency resolutions over the entire time-frequency plane. However, a slight difference can be discerned in the time-course of the component at $f_c/2$. In Fig. 1(c), the magnitude of this component goes to zero twice in the time interval between 90 and 370 ms, whereas in Fig. 1(e) it exists continuously. This is because the Morlet wavelet minimizes the product of the time and frequency resolutions whereas the AM wavelet does not. Since the frequency resolution of the two CWTs has been chosen to be identical everywhere, this implies that the time resolution of the AM-wavelet-based CWT is slightly inferior over the entire time–frequency plane.

Unlike the Morlet wavelet, however, the AM-based wavelet can be made strictly admissible by selecting f_c to be an integral multiple of f_m. However, this is more of theoretical interest than practical benefit in the present setting.

The $STFT$ presented in Figs. 1(f) and 1(g) is similar to the CWT. It has been chosen to have the same frequency resolution (49.7 Hz) as the CWTs at the carrier frequency, 756 Hz. However, unlike the CWTs, the widths of the spectral components are constant across frequency. For the $STFT$, both the time and frequency resolutions are independent of frequency, whereas for the CWT the frequency resolution improves (at the expense of the time resolution) as the frequency decreases. Thus, the Morlet-wavelet CWT in principle provides a better estimate of the frequency components below f_c. The $STFT$, on the other hand, provides superior frequency resolution for high frequencies.

We have also used the CWT and the $STFT$ in the analysis of velocity responses measured at lower sound pressure levels [2]-[5]. At the lowest sound intensities only multiples of the carrier frequency are present. As the intensity increases, half-harmonic components appear, followed by quarter-harmonic components at the highest levels. This pattern is indicative of a period-doubling route to chaos.

4. CONCLUSION

Both CWT and $STFT$ techniques are useful for analyzing the time-varying responses of sensory cells in the cochlea. For the CWT, wavelet bases with controllable relative bandwidth should be used inasmuch as they allow selected frequency resolution to be chosen at an arbitrary analysis frequency. The Morlet wavelet and AM wavelet are about equally as effective. The information provided by time–frequency and time–scale analysis has narrowed the range of nonlinear oscillators admissible as mathematical models for cochlear function.

5. ACKNOWLEDGMENTS

This work was supported by the Office of Naval Research under Grant N00014-92-J-1251, the National Institutes of Health through NIDCD Program Project Grant DC00316, the Emil Capita Foundation, the Swedish Medical Research Council (02461), the Magnus Bergvall Foundation, and the Tysta Skolan Foundation.

6. REFERENCES

[1] International Team for Ear Research (ITER), *Cellular Vibration and Motility in the Organ of Corti, Acta Otolaryngol. (Stockholm)*, Supplement 467, pp. 1–279, 1989.

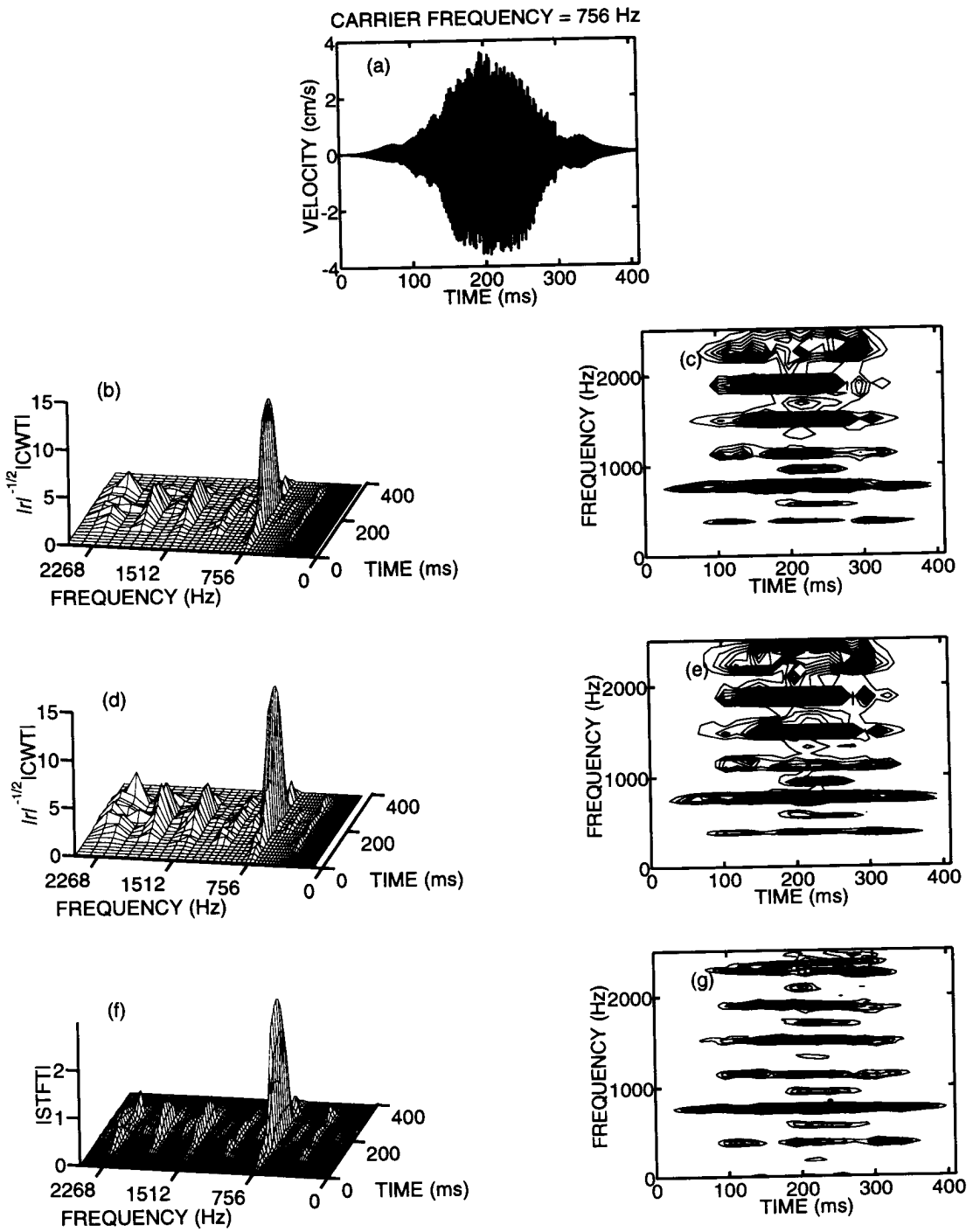

Figure 1: Velocity response of an outer hair cell in the third turn of a guinea-pig temporal-bone preparation to an *AM* pulse with carrier frequency $f_c = 756$ Hz. (a) Time waveform of the response. (b) 3D plot of the modified *CWT* magnitude (calculated using the Morlet wavelet) of the velocity response shown in (a). (c) Same modified *CWT* magnitude as shown in (b), but with 80 equally spaced contour lines joining points of constant magnitude. (d) 3D plot of the modified *CWT* magnitude (calculated using the AM wavelet) of the velocity response shown in (a). (e) Same modified *CWT* magnitude as shown in (d), but with 80 equally spaced contour lines. (f) 3D spectral plot of the *STFT* magnitude of the velocity response shown in (a). (g) Same *STFT* magnitude as shown in (d), but now plotted in 2D contour format, with 80 equally spaced contour lines.

REFERENCES

[1] International Team for Ear Research (ITER), *Cellular Vibration and Motility in the Organ of Corti, Acta Otolaryngologica (Stockholm),* Supplement 467, pp. 1–279, 1989.

[2] M. C. Teich, C, Heneghan, S. M. Khanna, Å. Flock, L. Brundin, and M. Ulfendahl, "Analysis of dynamical motion of sensory cells in the organ of Corti using the spectrogram," in *Biophysics of Hair Cell Sensory Systems*, H. Duifhuis, J. W. Horst, P. van Dijk, and S. van Netten, Eds., Singapore: World Scientific, 1993.

[3] C. Heneghan, M. C. Teich, S. M. Khanna, and M. Ulfendahl, "Nonlinear dynamical motion of cellular structures in the cochlea," *Proc. SPIE,* vol. 2036, pp. 183–197, 1993.

[4] C. Heneghan, S. M. Khanna, Å. Flock, M. Ulfendahl, L. Brundin, and M. C. Teich, "Investigating the nonlinear dynamics of cellular motion in the inner ear using the short-time Fourier transform and the continuous wavelet transform," *IEEE Trans. on Sig. Proc.*, to be published.

[5] M. C. Teich, C. Heneghan, S. M. Khanna, Å. Flock, L. Brundin, and M. Ulfendahl, "Investigating Routes to Chaos in the Inner Ear Using the Short-Time Fourier Transform and the Continuous Wavelet Transform," *Annals of Biomedical Engineering,*, to appear, Fall 1994.

[6] O. Rioul and M. Vetterli, "Wavelets and Signal Processing," *IEEE Signal Processing Magazine* vol. 8, no. 4, pp. 14–38, 1991.

[7] D. L. Jones and R. G. Baraniuk, "Efficient approximation of the Continuous Wavelet Transform," *Electronics Letters*, vol. 27, no. 9, pp.748–750, April 1991.

[8] A. Grossmann, R. Kronland-Martinet, and J. Morlet. "Reading and understanding continuous wavelet transforms," . in *Wavelets: Time-Frequency Methods and Phase Space*, 2nd Ed., J. M. Combes, A. Grossmann, and Ph. Tchamitchian, Eds., New York: Springer-Verlag, 1989/1990, pp. 2–20.